Supplementary information

for

Nitrogen-Vacancy Cobalt Nitride Nanoparticle Coated Hollow Carbon Spheres as Electrocatalysts for Lithium–Sulfur Batteries

Hao Wu,[a] Hao Jiang,[a] Yongqiang Yang,[a] Chenyi Hou,[a] Haitao Zhao,[b,c] Ru Xiao,[*a] and Hongzhi Wang[*a]

Experimental Details

Material Synthesis

Aqueous ammonia, dopamine, HNO_3, H_2SO_4, HF, 2-methylimidazole, tetraethoxysilane, n-octadecyltrimethoxysilane and Tris(hydroxymethyl)aminomethane were purchased from Aladdin Shanghai Biochemical Technology Co., Ltd. $CoCl_3 \cdot 6H_2O$ and solid sulfur powderswere purchased from Alfa Aesar. Poly(vinylidene fluoride) (PVDF), N-methyl-2-pyrrolidone (NMP) and acetylene black were purchased from Solvay (Shanghai) Co., Ltd., Aladdin Shanghai Biochemical Technology Co., Ltd. and Royal Dutch Shell, respectively.

Synthesis of silica templates: All chemicals used in this study were of analytical grade. Preparation of silica templates was described in a previous report.[1] Typically, Aqueous ammonia (32 wt%, 5 mL) was added into the 100 mL 75% ethanol. Then, 6 mL of tetraethoxysilane was added in the above solution and stirred for 1 hour at room temperature to make silica nanoparticle cores. To increase the roughness of silica sphere, the tetraethoxysilane/n-octadecyltrimethoxysilane mixture (6 mL: 6 mL) was added in the above solution, stirred for 1 min and keep 3 h at room temperature for coating a homogeneous layer on the surface of silica. The above powder was obtained through centrifugation, vacuum drying and calcination in air for 4 h at 500℃ to form the porous silica templates.

Synthesis of hollow carbon spheres: 0.9 g of silica template was dispersed in 900 mL water and stirred, sonicated for 0.5 h. 0.3 mg of Tris(hydroxymethyl)aminomethane and 0.54 mg of dopamine were added into the above solution and stirred for 24 hours, respectively. The polydopamine coated silica particles were obtained by centrifugation under 8500 rpm/min, which was then heated at 800℃ for 3 h to carbonize the dopamine under Argon. The obtained carbon coated silica was etched by 40 mL HF mixture solution (10 mL HF: 30 mL water) for 5 h to give the hollow carbon spheres.

Acidification of hollow carbon spheres: In order to increase the surface functional groups and adsorption capacity of carbon spheres, 0.1g hollow carbon sphere were refluxed with HNO_3 and H_2SO_4 mixture (1/3, v/v, 8 mL) at 70℃ for 6 h. The resulting powder were washed with deionized water and then centrifuged until the pH of the suspension was approximately 7.

Synthesis of hollow $Co_{5.47}Nx$-C spheres: 0.1 g acidate carbon spheres were added into 10 mL 3.5M $CoCl_3$ and stirred for 3 h under room temperature. To avoid the redundant precursor, synthesis process of ZIF-67 precursors was performed with a typical vacuum filtration setup by adding the colorless 2-methylimidazole solution on top of the acidate carbon spheres-Co^{3+}solution placed on a glass filter, while controlling the vacuum pressure to obtain ZIF-67-carbon spheres. The above powder was vacuum drying and calcination in ammonia for 2 h at 600 ℃ form the hollow $Co_{5.47}Nx$-C spheres.

Synthesis of $Co_{5.47}N$: 4 mmol $CoCl_3 \cdot 6H_2O$ and 12 mmol hexamethylenetetramine were dissolved in 30 ml ultra-pure water under a constant stirring for 30 min. Then, the suspension was transferred to a 50 ml Teflon lined

autoclave and heated at 100℃ for 10 h. After that, the e as-prepared CoO above was placed in a ceramic crucible and calcined at 300℃ for 2 h under NH_3 flow form the $Co_{5.47}N$.[2]

Preparation of the $Co_{5.47}Nx$-C spheres/S Cathode: To impregnate the sulfur into the hollow $Co_{5.47}Nx$-C spheres, the solid sulfur powders and hollow spheres were mixed and heated at 155℃ for 20 h in a sealed vacuum tube. To prepare the cathodes, sulfur-based materials were first mixed with carbon black and PVDF (7:2:1 by weight) in N-methyl-2-pyrrilidonesolvent through grind by using a bowl mill. The slurry was then spread on an aluminum foil and roll-pressed to produce electrode films under 50℃ overnight. The average sulfur loading is 1.8~2.2 mg cm^{-2}

Characterization techniques

X-ray diffraction (XRD) measurements were conducted on a Rigaku D/max 2550 V diffractometer using Cu KR radiation at a wavelength of 1.5406 Å. Scanning electron microscope (SEM) was performed with a SU-8010 field emission SEM. Transmission electron microscope (TEM), and elemental mapping were carried out using a FEI Tecnai G2 F20 TEM with 200 kV. X-ray photoelectron spectroscopy (XPS) measurements were performed using a Kratos Axis Ultra multi-functional X-ray photoelectron spectroscope and the typical detection depth is ~5 nm. All XPS spectra were corrected using the C 1s line at 284.7 eV. Raman spectroscopy (inVia-Reflex with an excitation wavelength of 785 nm). Nitrogen adsorption and desorption isotherms at 77.3 K were carried out with a ASAP 2020 physisorption analyzer (USA). Thermogravimetric analysis (TGA, Labsys NETZSCH TG-209) was used to investigate the sulfur content of the cathode. It was carried out in air atmosphere from 50 to 600 °C at a heating rate of 10 °C min^{-1}.

Coin cell assembly and test

2032 coin-type cells were used for all tests. The coin cells were assembled with the $Co_{5.47}Nx$-C spheres/S cathode and the pure lithium metal anode along with a Celgard 2500 separator. The cell was using lithium bis–trifluoromethanesulfonylimide LiTFSI (1M in DOL/DME) containing $LiNO_3$ (0.4M) as electrolyte. The discharge and charge measurement of the cells were performed on a LAND CT2001A electrochemical workstation between 2.8 and 1.7 V at room temperature. The cycling voltammogram (CV) test of the batteries were performed by a CHI660D electrochemical workstation with the potential range of 1.7-2.8 V. Electrochemical Impedance Spectroscopy (EIS) of these batteries was test from 1 MHz to 0.1 Hz.

DFT calculations

All the first-principle calculations were performed on the basis of density functional theory (DFT) with the Vienna Ab-initio Simulation Package (VASP 5.3) code, using the Perdew, Burke, and Ernzerhof (PBE).[3,4] The Kohn-Sham orbitals are expanded in a plane-wave basis set, and 400 eV is set as the energy cutoff for local geometry optimization. Standard projected augmented-wave potentials are utilized for the electron-iron interaction. Hydrogen and carbon atoms are calculated with 1 and 4 electrons, respectively. A 3 × 3 × 1 Monkhorst-Pack k-point mesh is used for bulk calculation and 1 × 1 × 1 k-point grid is set for single molecule calculations. Gaussian smearing is utilized as Methfessel and Paxton smearing and applied to zeroth order, with a smearing width of 0.1 eV. The calculations are performed spin-unrestricted due to nonzero bulk magnetic moments. The van der Waals density functional corrections are used in this work.
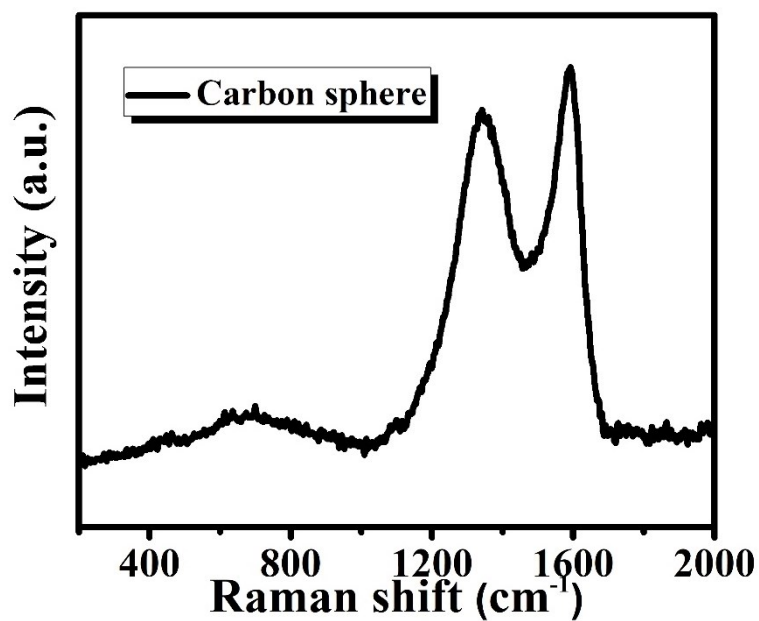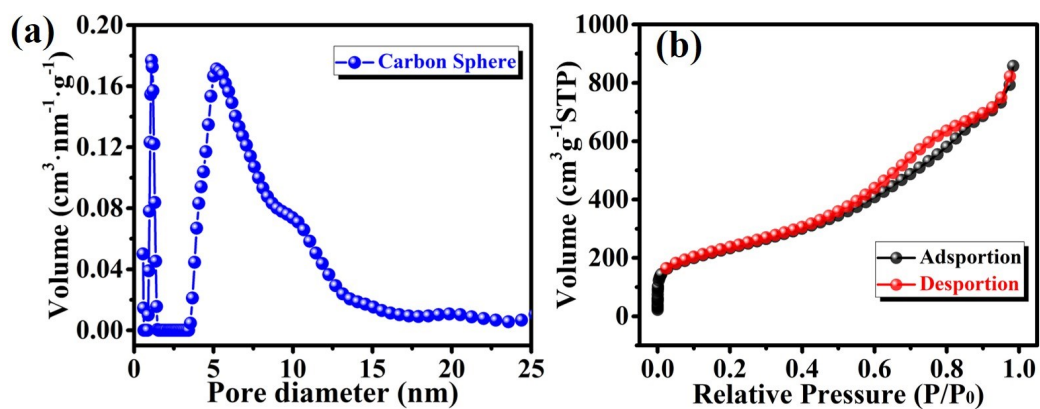
Figure. S1 The Raman spectra of C spheres

Figure. S2 (a) the average pore size distribution and (b) the nitrogen adsorption/desorption isotherms of the C spheres
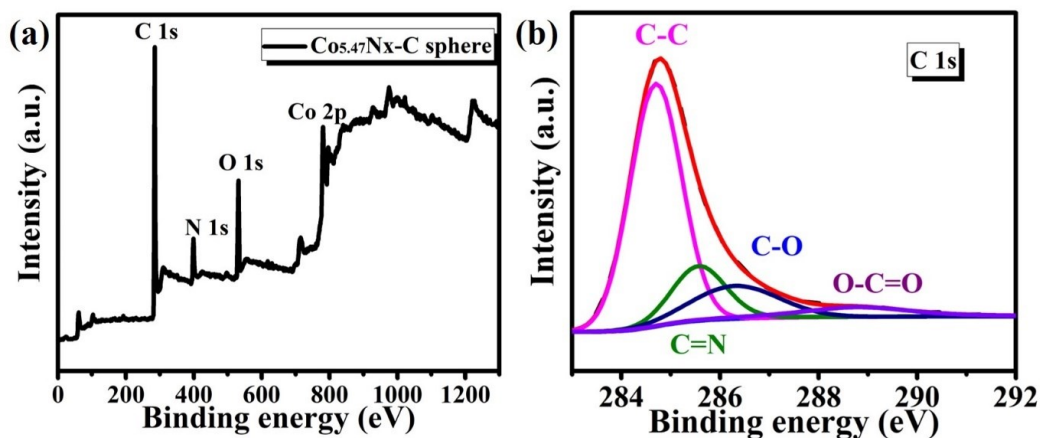
Figure. S3 (a) XPS full scan and (b) C 1s XPS spectrum of $Co_{5.47}Nx$-C sphere

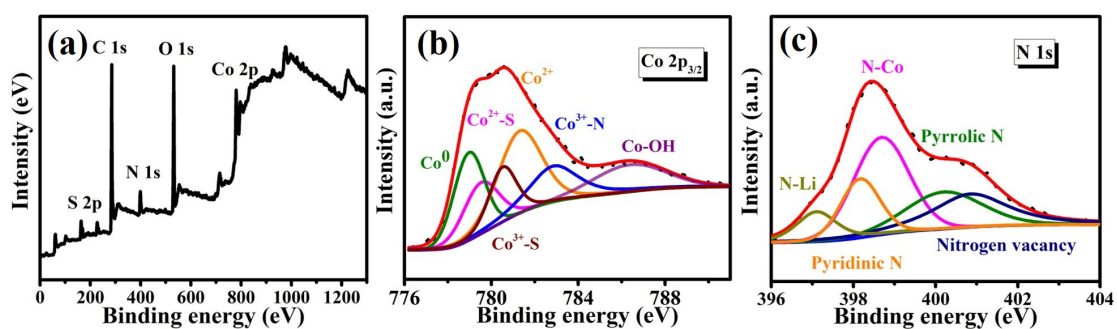Figure. S4 (a) the XPS full scan, (b) high-resolution XPS of Co $2P_{3/2}$ and (c) of N 1s spectra for $Co_{5.47}Nx$-C sphere-Li_2S_6.

S$_8$ on Co$_{5.47}$Nx   Li$_2$S$_8$ on Co$_{5.47}$Nx   Li$_2$S$_6$ on Co$_{5.47}$Nx

Li$_2$S$_4$ on Co$_{5.47}$Nx   Li$_2$S$_2$ on Co$_{5.47}$Nx   Li$_2$S on Co$_{5.47}$Nx
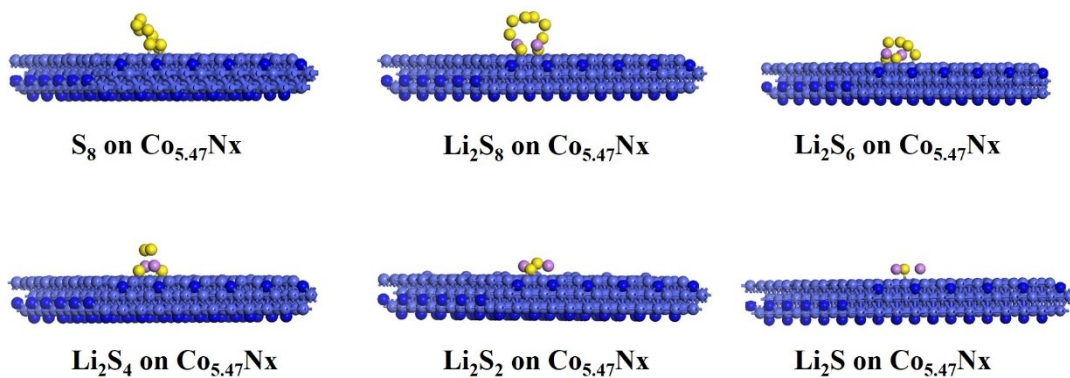
Figure. S5 the calculated interaction energy (Eb) of Li$_2$Sx (x = 1, 2, 4, 6 or 8) species and S$_8$ on the top views of Co$_{5.47}$Nx crystals.
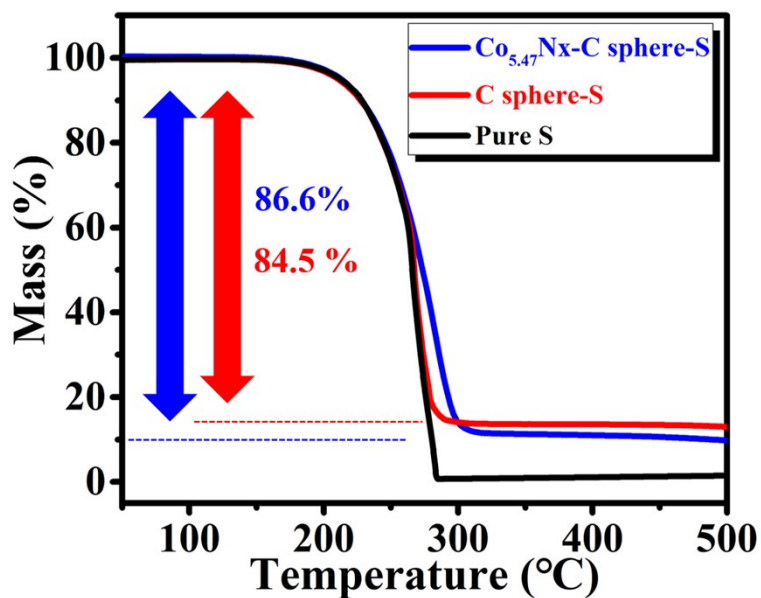
Figure. S6 the TG curves of Co$_{5.47}$Nx-C sphere/S, C sphere/S and pure S under air.
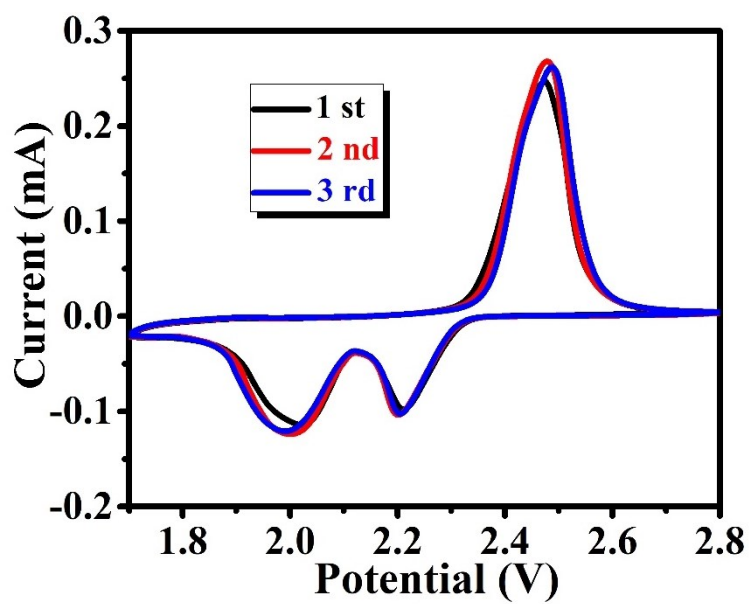
Figure. S7 The CV curve of C sphere/S cathode at first three cycles under 0.05 mv/s.
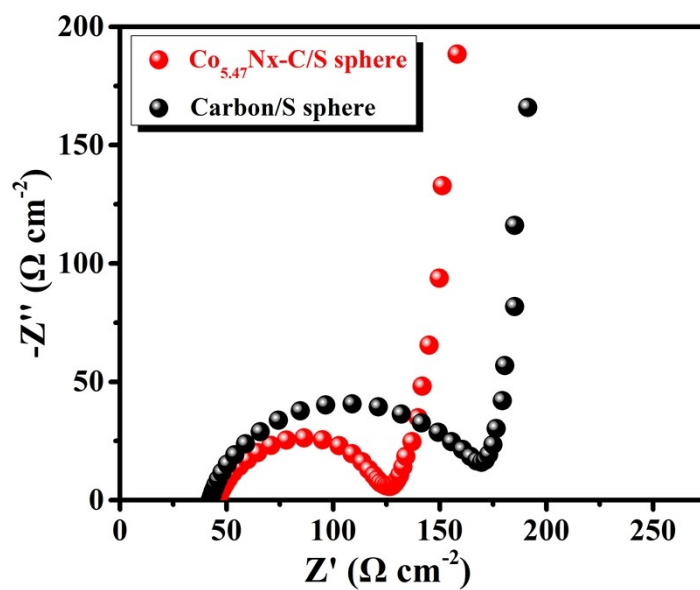
Figure. S8 the electrochemical impedance spectra of $Co_{5.47}Nx$-C sphere/S and C sphere/S cathode.
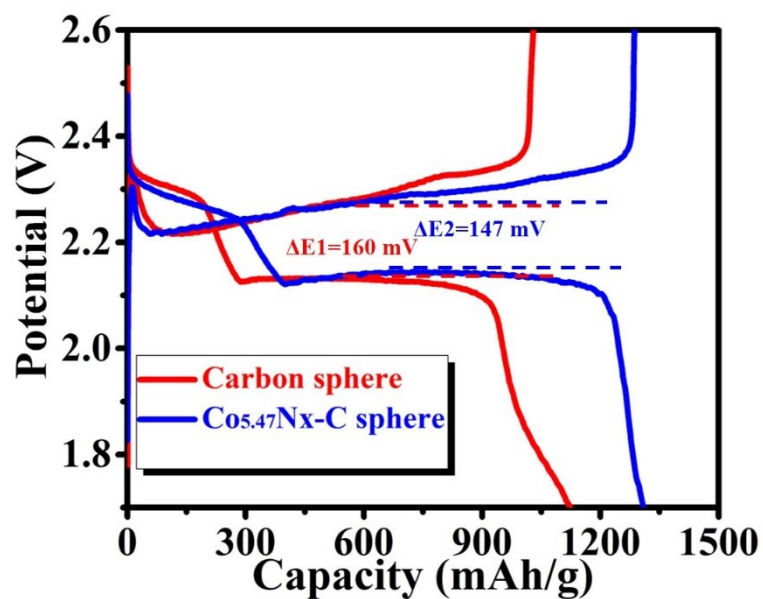
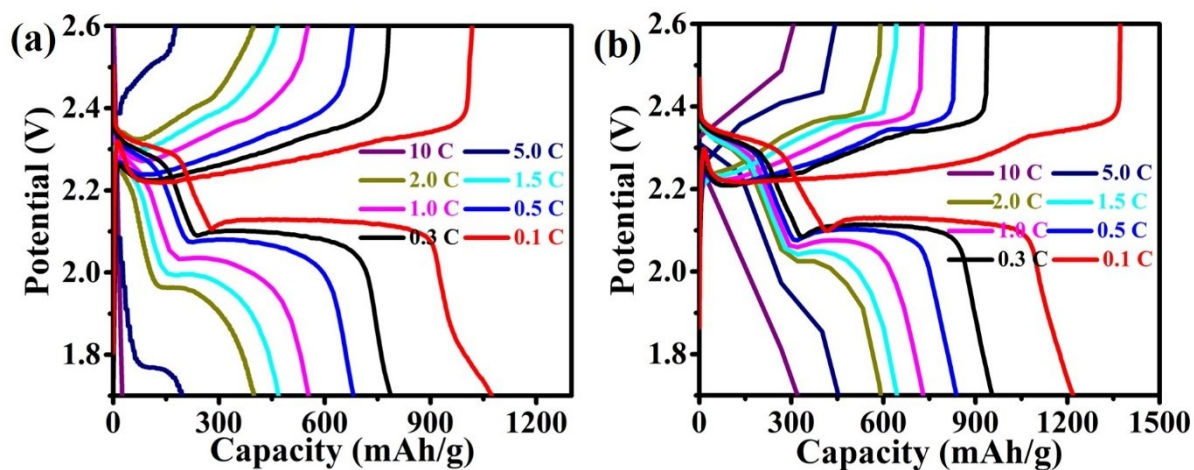Figure. S9 the charge/discharge curve of $Co_{5.47}Nx$-C sphere/S and carbon sphere/S cathode at 0.1 C

Figure. S10 the charge/discharge curve of $Co_{5.47}Nx$-C sphere/S and C sphere/S at different rating.

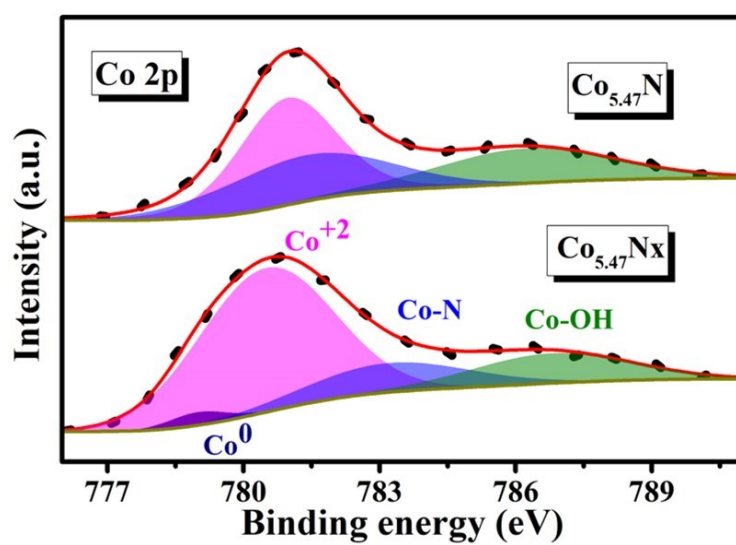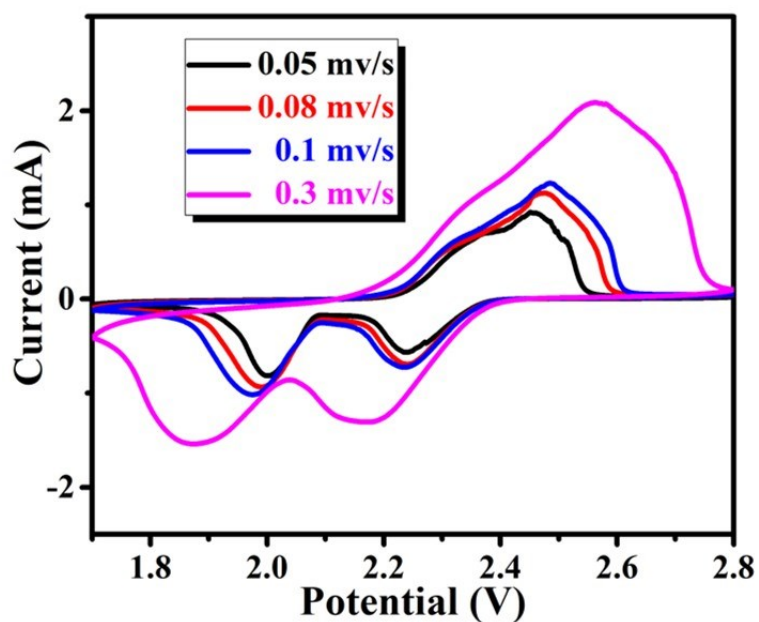Figure. S11 The high-resolution XPS of Co 2P$_{3/2}$

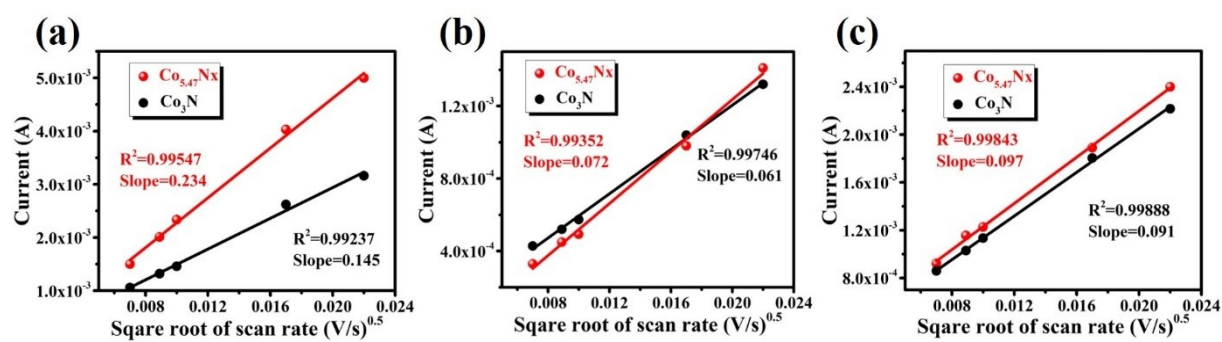Figure. S12 The CV curves of Co$_{5.47}$N/S from 0.05 mv/s to 0.3 mv/s

Figure. S13 The peak currents versus square root of scan rates of $Co_{5.47}Nx/S$ and Co_3N/S, (a) peak A, (b) peak B and (c) peak C

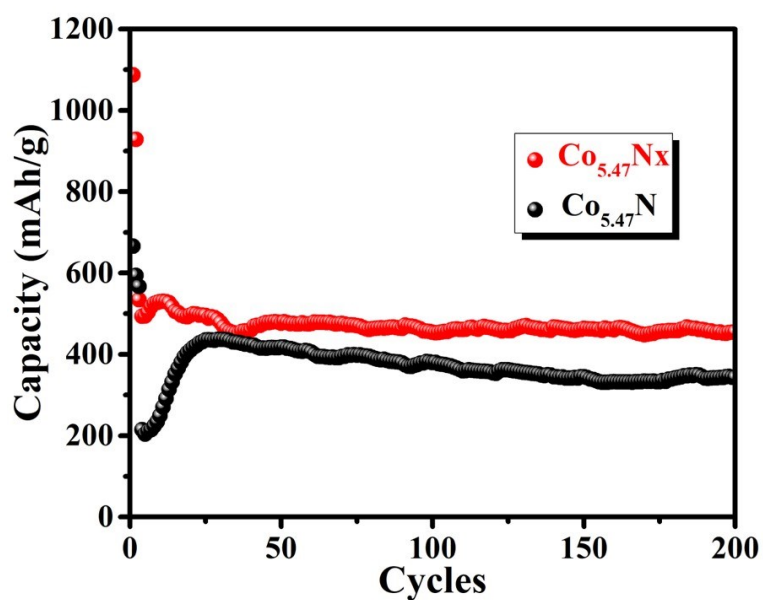Figure. S14 The cycling performance and coulombic efficiencies at 0.5 C for nitrogen-vacancy $Co_{5.47}Nx$ /S and $Co_{5.47}N/S$ without nitrogen vacancies, respectively.

Notes and references

1 W. D. Zhou, C. M. Wang, Q. L. Zhang, H. D. Abruña, Y. He, J. W. Wang, S. X. Mao and X. C. Xiao, *Adv. Energy Mater*., 2015, 5, 1401752.

2 L. Q. Yang, Y. g Liu, L. Wang, Z. J. Zhao. C. J. Xing, S. H. Shi, M. L. Yuan, Z. M. Ge, and Z. Y. Cai, *Catal. Lett.*, 2019, **149**, 3111–3118

3 G. Kresse, and J. Furthmüller, *Comput. Mater. Sci.,* 1996, **6**, 15-50.

4 G. Kresse, and J. Furthmüller, *Phys. Rev. B*, 1996, **54**, 11169.